Available online at www.sciencedirect.com
SCIENCE DIRECT®
Bioorganic & Medicinal Chemistry
Bioorganic & Medicinal Chemistry 13 (2005) 5164–5170

Optically active cantharidin analogues possessing selective inhibitory activity on Ser/Thr protein phosphatase 2B (calcineurin): Implications for the binding mode

Yoshiyasu Baba,[a] Nozomu Hirukawa[a] and Mikiko Sodeoka[a,b,*]

[a]*Institute of Multidisciplinary Research for Advanced Materials, Tohoku University, 2-1-1 Katahira, Aoba, Sendai, Miyagi 980-8577, Japan*
[b]*RIKEN (The Institute of Physical and Chemical Research), 2-1 Hirosawa, Wako, Saitama 351-0198, Japan*

Received 24 March 2005; revised 10 May 2005; accepted 10 May 2005
Available online 13 June 2005

This article is dedicated to Professor Koji Nakanishi for his truly outstanding contributions to organic, biorganic, and natural products' chemistry on the occasion of his receiving the 2004 Tetrahedron Prize and his 80th birthday.

Abstract—Cantharidin is well known as a potent serine/threonine protein phosphatase 1 and 2A (PP1 and PP2A) inhibitor, with less potent inhibitory activity for PP2B, which regulates T-cell proliferation. We synthesized and evaluated four optically pure stereoisomers of 1-substituted norcantharidin analogues. The absolute stereochemistry of each stereoisomer was determined based on X-ray crystal structure analysis. Remarkably, optically active cantharidin analogues having (1*S*)-configuration showed selective inhibition of PP2B, without inhibiting PP1 or PP2A.

1. Introduction

Cantharidin (**1**) (Fig. 1) was originally identified as a biologically active constituent of the dried body of Chinese blister beetle (*Mylabris phalerata* or *M. cichorii*) and Spanish fly.[1] Cantharidin inhibits Ser/Thr protein phosphatases 1 (PP1) and 2A (PP2A) (PP1 IC_{50} = 473 nM; PP2A IC_{50} = 40 nM), which have key roles in many cellular processes, such as regulation of cell proliferation and differentiation.[2] In contrast, cantharidin inhibits Ser/Thr protein phosphatase 2B (PP2B) very weakly (IC_{50} = >30,000 nM). There have been numerous studies of cantharidin analogues aimed at the discovery of potent and selective inhibitors of PP1 and PP2A,[3] and some candidate inhibitors of Ser/Thr protein phosphatase 2B (PP2B) have also been reported.[4]

PP2B (calcineurin) is a calcium and calmodulin-regulated phosphatase, which catalyzes dephosphorylation of NF-AT (nuclear factor of activated T-cells), leading to T-cell lymphocyte activation.[5] Recently, PP2B has also attracted attention as a target enzyme for treatment of heart failure.[6] The therapeutic immunosuppressants cyclosporin A and FK506 bind with high affinity to cytoplasmic receptors termed immunophilins (immunosuppressant binding proteins), and these binding complexes inhibit PP2B, leading to the suppression of T-cell proliferation.[7] Remarkably, these immunosuppressants cannot directly inhibit PP2B; formation of the immunophilin complex is essential. Thus, we started a project to find a selective inhibitor of PP2B that would act directly without requiring immunophilins,[8] as a biological tool for studies of PP2B, and also as a candidate therapeutic agent. Initially, we focused on PP2B-selective analogues of cantharidin.

Recently, we found a highly selective catalytic site-directed inhibitor of PP2B, the cantharidin analogue **4** (IC_{50} = 7 μM), which shows negligible inhibition of PP1 and PP2A.[4a] Our strategy for the development of a selective PP2B inhibitor was as follows. Based on the structure–activity relationships (SARs) between the cantharidin derivatives and all three PPs, a 'core' structure that interacts with the highly conserved catalytic site

Keywords: PP2B; Calcineurin; Cantharidin; Inhibitor; Optically active.
* Corresponding author. Tel./fax: +81 22 217 5601; e-mail: sodeoka@tagen.tohoku.ac.jp

0968-0896/$ - see front matter © 2005 Elsevier Ltd. All rights reserved.
doi:10.1016/j.bmc.2005.05.013

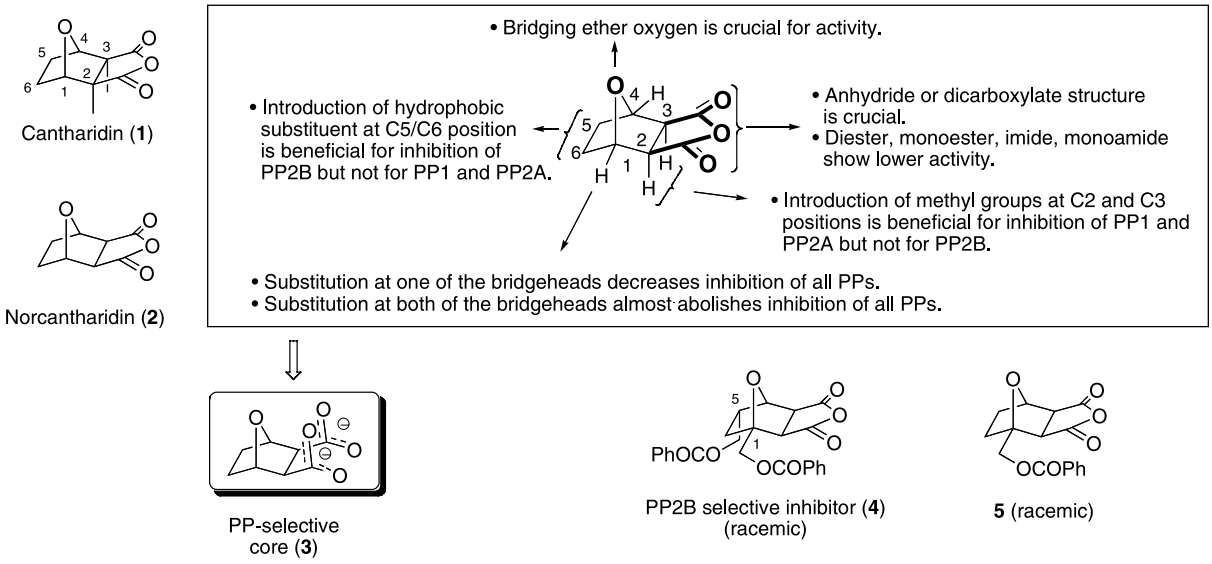

Figure 1. Cantharidin analogues and summary of their reported structure–activity relationships.

of PPs (PP1, 2A, and 2B) as a Ser/Thr phosphopeptide mimic was identified. The SARs determined in our and other laboratories are summarized in Figure 1.[3,4] Since the data indicated that the anhydride/dicarboxylate structure at the C2/C3 positions and the bridging ether oxygen are critical for the inhibition of all PPs, norcantharidin dicarboxylate (*exo*, *exo*-7-oxabicyclo[2.2.1]heptane-2,3-dicarboxylate, **3**) was determined to be a suitable 'core' structure for PP inhibitors (Fig. 1). Then, a binding model of the 'core' structure and the catalytic site of PP2B was constructed by using computational docking techniques (Fig. 2A). Finally, the PP2B-selective inhibitor **4** was obtained by the introduction of substituents that can interact with unique regions of PP2B onto the 'core' structure, according to the binding model.[4a,9] In our model, the critical ether oxygen of the oxabicyclo[2.2.1]heptane skeleton is hydrogen-bonded to an Arg residue (Arg254 of PP2B, corresponding to Arg221 of PP1) (O-Arg-type binding mode) (Fig. 2B). In contrast, Chamberlin and co-workers proposed different binding models of cantharidic acid with PP1 and PP2A.[10] In these models, the cantharidic acid seems to face the opposite direction, forming a hydrogen bond between the ether oxygen and Tyr residue (Tyr272 of PP1 and Tyr261 of PP2A, respectively, corresponding to Tyr 311 of PP2B) (O-Tyr-type binding mode) (Fig. 2B). Tatlock et al. also reported a binding model of a 5-substituted norcantharidin derivative with PP2B,[4c] and their model seems to be basically similar to the O-Tyr-type binding mode. In fact, our further molecular modeling studies on the interaction between the simple norcantharidin carboxylate core and PP2B suggest the existence of several possible binding modes. Introduction of a substituent into the 'core' structure might fix the binding mode of the compound. Here, we focus on substitution at the C1-position for this purpose. In the O-Arg-type binding mode, the direction of one of the bridgehead-hydrogen (H_R) would be blocked by the loops Glu282-Gln284 and Phe306-Ala308, while the other bridgehead-hydrogen (H_S) seems to be facing the groove between the α-helix$_{156–160}$ and loop$_{251–256}$ (Fig. 2A). In contrast, H_S seems to be blocked in the

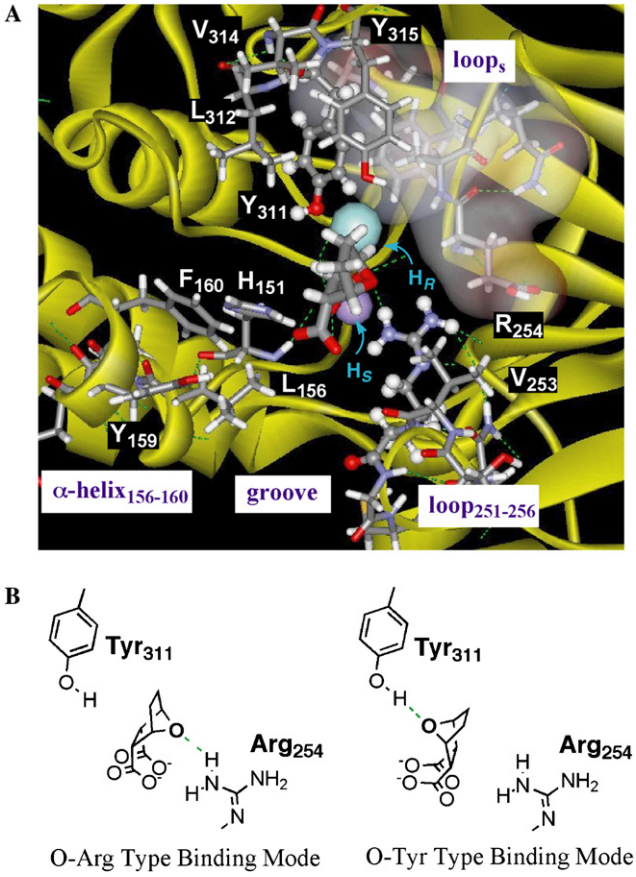

Figure 2. Binding model of **3** and PP2B. (A) Compound **3** is represented as thick sticks. Arg254 and Tyr311 are represented in ball and stick form. Amino acid residues surrounding the groove (156–160 and 251–256), His151, Leu312, and Tyr315 are shown in stick form. The amino acid residues (282–284 and 306–308) near one of the bridgehead-hydrogen (H_R) are indicated in stick form with surfaces. (B) Schematic drawings of the two types of binding modes.

O-Tyr-type binding mode. We have already reported that mono-substitution at the C1 position (such as in racemic **5**) decreased inhibition of all PPs, and di-substitution at the C1 and C4 positions, even with a small methyl group, almost abolished inhibitory activity toward all PPs.[4a,b] Thus, we speculated that only one of the enantiomers of the mono-C1-substituted derivative might be responsible for the inhibition of PPs. The preferred binding mode (O-Arg-type or O-Tyr-type) of each PP could be determined by comparison of the inhibitory activities of the optically pure enantiomers. To our knowledge, however, no optically pure cantharidin analogue having a chiral center on its bicyclic skeleton has been examined for PP-inhibitory activity.[11] To clarify the relationships between the absolute configuration at the C1 position of cantharidin analogues and the inhibitory activity toward each PP, we synthesized optically pure C1-substituted derivatives and evaluated their inhibitory activities.

2. Results

2.1. Synthesis of chiral 1-benzoyloxyethylnorcantharidin analogues

Since attempts to separate the enantiomers of **5** were unsuccessful, we synthesized the 1-benzoyloxyethyl derivatives instead of **5**. Optically pure (*R*)-1-(2-furyl)ethanol was selected as a chiral source and was transformed to its benzoyloxyethyl derivative (*R*)-**6**. Compound (*R*)-**6** was subjected to Diels–Alder reaction with maleic anhydride at room temperature (Scheme 1). Hydrogenation of the crude adducts gave 1-substituted cantharidin analogues, (1*S*,10*R*)-**7** and (1*R*,10*R*)-**8**, as a diastereomixture. Separation of the diastereomers was achieved by fractional recrystallization, and optically pure (1*S*,10*R*)-**7** and (1*R*,10*R*)-**8** were obtained. Optically pure (1*S*,10*S*)-**10** and (1*R*,10*S*)-**11** were synthesized from (*S*)-1-(2-furyl)ethanol by the same method.

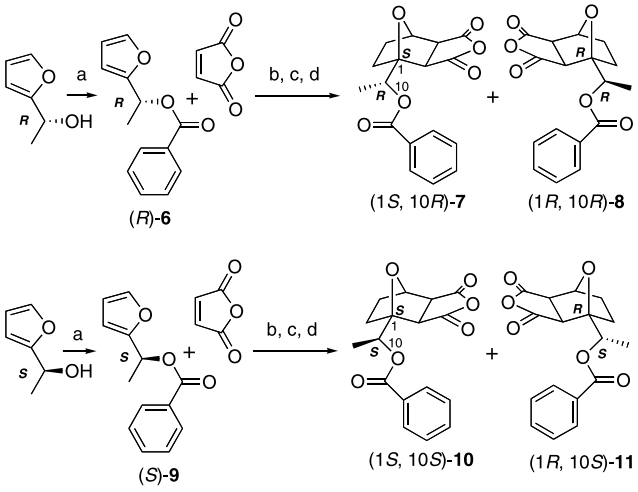

Scheme 1. Synthesis of chiral norcantharidin analogues. (a) BzCl, Et_3N, DMAP, CH_2Cl_2; (b) neat, rt, (c) H_2, 10% Pd–C, THF; (d) separation of the diastereomers.

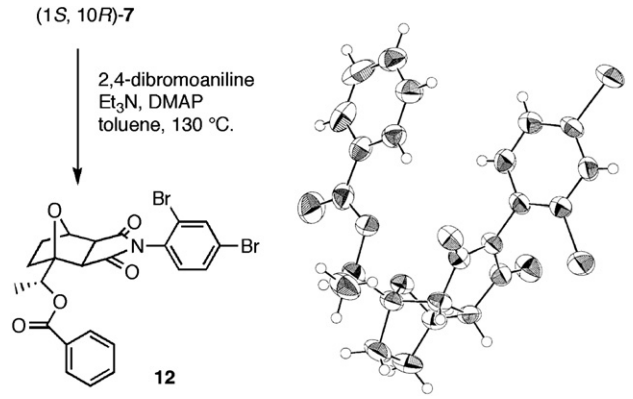

Figure 3. Preparation of **12** and ORTEP view of its crystal structure. The crystal structural information has been deposited in the Cambridge Crystallographic Data Center (deposition number CCDC 267159).

The C1 stereochemistry of the chiral cantharidin analogue **7** having 10*R* side chain chirality was determined to be (*S*) by X-ray crystal structure analysis of the imide derivative **12**, which was prepared from **7** by reaction with 2,4-dibromoaniline in the presence of Et_3N and DMAP. An ORTEP view of the crystal structure of **12** is shown in Figure 3. The absolute stereochemistries of the other stereoisomers (**8**, **10**, and **11**) were also automatically assigned.

2.2. Inhibition assay[4a,12]

Four chiral norcantharidin analogues were screened for their ability to inhibit PP1, PP2A, and PP2B at concentrations of 100 μM and 1 mM (Fig. 4). The absolute stereochemistry at the C1 position had a remarkable effect on the inhibitory activity toward PP1 and PP2A. Irrespective of the side chain stereochemistry, the (1*R*)-isomers **8** and **11** inhibit PP1 and PP2A, whereas the (1*S*)-isomers **7** and **10** have negligible inhibitory activity for PP1 and PP2A. Interestingly, however, PP2B was inhibited by all four stereoisomers, **7**, **8**, **10**, and **11**.

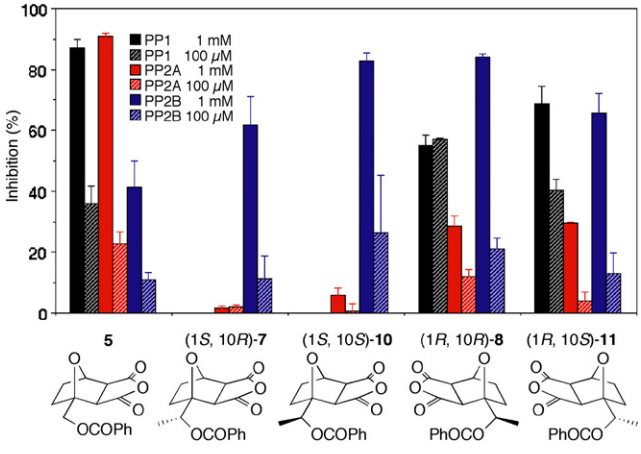

Figure 4. Inhibitory activities of chiral cantharidin analogues (**7**, **8**, **10**, and **11**). Black, red, and blue bars represent inhibition of PP1, PP2A, and PP2B, respectively. Solid bars and striped bars indicate inhibition at 1 mM and 100 μM drug concentrations, respectively. Error bars indicate standard deviations ($n = 3$).

Thus, the chiral norcantharidin analogues **7** and **10** having (*S*)-absolute configuration at the C1 position showed excellent selectivity for PP2B. It is also noteworthy that all four stereoisomers are PP2B-selective, while the racemic **5** preferred PP1/PP2A.[4a]

3. Discussion

Based on the observed clear difference of PP2B selectivity depending on the absolute stereochemistry at the C1 position, we speculate that PP1 and PP2A favor the O-Tyr-type binding mode, whereas PP2B can accept two different types of binding modes (Fig. 2B). PP2B binds all four stereoisomers and slightly prefers **8** and **10** over **7** and **11**. Figures 5A and 5B show binding models of the (1*R*,10*R*)-isomer **8** and (1*S*,10*S*)-isomer **10** to PP2B, respectively. In both models, the carboxylate groups are located at the bottom of the catalytic site and interact with conserved basic residues, but the orientation of the ether oxygen is different depending on the stereochemistry at the C1 position. The bulky benzoyloxyethyl group is located in the groove, and, as a result, the bridging ether oxygen faces in opposite directions in the enantiomers. In contrast, PP1 and PP2A bind only the (1*R*)-enantiomers **8** and **11**, suggesting that PP1 and PP2A may prefer a binding mode like that in Figure 5A. Actually, the shapes of the groove are different between the reported crystal structures of PP2B[13] and PP1,[14] mainly due to the difference of structure at two regions, an α-helix (residues 156–160 of PP2B and 130–134 of PP1) and a loop (251–256 of PP2B and 218–223 of PP1) (Figs. 5, 5C, and 6D). In both models, the benzoyloxyethyl group is located between them, and the difference of these regions may contribute to the observed selectivity. Of course, there are many other possible binding modes, and, to confirm the true binding mode of each stereoisomer, X-ray analyses of the complexes will be necessary.

We have already reported that introduction of a hydrophobic substituent at the C5 position of **5** greatly improves the inhibition of PP2B.[4a] In fact, 1-benzoyloxymethyl-5-(4-phenylbutanoyl)oxymethyl-norcantharidin showed higher PP2B-inhibitory activity than the dibenzoyloxymethyl derivative **4**,[4a] but, in the case of the racemic compounds, the selectivity was not as high as that of compound **4**. The observed high PP2B

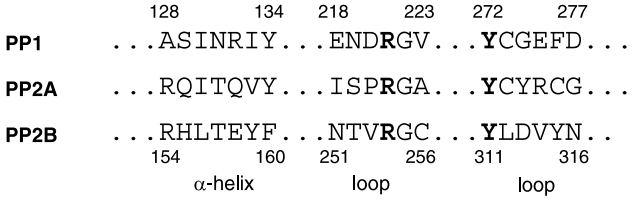

Figure 6. Comparison of the amino acid residues surrounding the catalytic site.

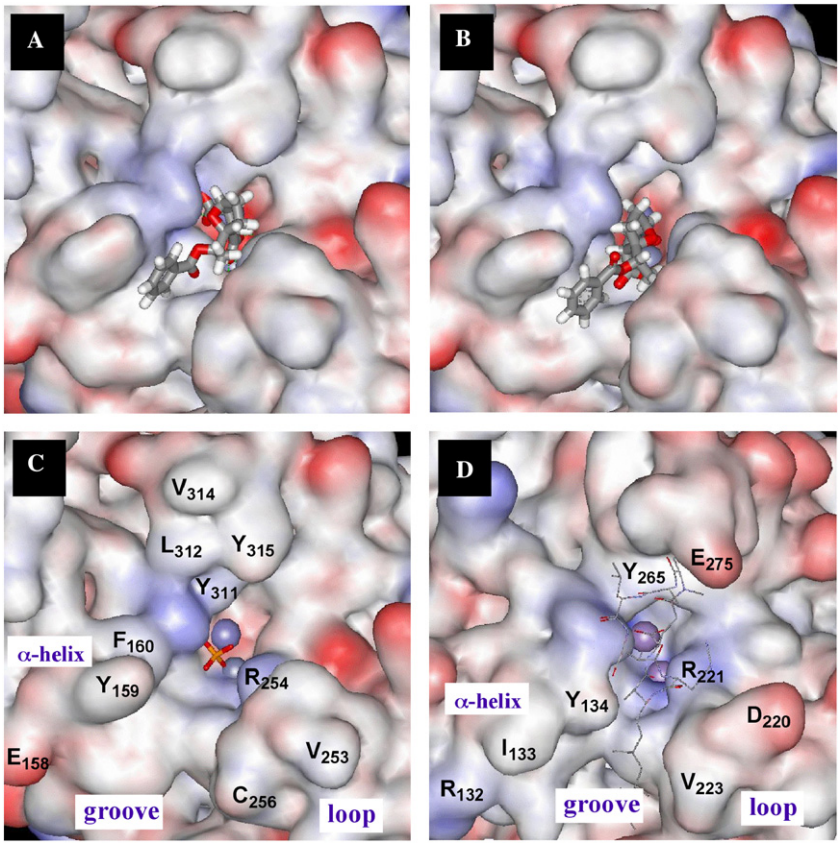

Figure 5. (A) Binding model of (1*R*,10*R*)-**8** and PP2B. (B) Binding model of (1*S*,10*S*)-**10** and PP2B. (C) Catalytic site structure of PP2B–phosphate complex (PDB ID: 1TCO).[13a] (D) Catalytic site structure of PP1–microcystin complex (PDB ID: 1FJM).[14a]

selectivity of the (1*S*)-enantiomer of the mono-substituted derivatives suggests that the (1*S*)-enantiomer of these disubstituted derivatives should also show high PP2B selectivity, if it could be synthesized in optically pure form. Efforts to synthesize optically pure 1,5-disubstituted norcantharidin derivatives are underway.

It is also noteworthy that introduction of a methyl group into the side chain increased the inhibition of PP2B and decreased the inhibition of PP1 and PP2A in all stereoisomers compared to the racemic parent compound **5**, suggesting that better inhibitors might be obtained by optimization of the C1 substituent.

4. Conclusion

A series of optically pure C1-substituted norcantharidin analogues have been synthesized, and the absolute stereochemistries were determined based on X-ray crystal structural analysis. The inhibitory activities of the four stereoisomers toward PP1, PP2A, and PP2B were measured and compared. The absolute stereochemistry of the C1 position was found to be important for the subtype selectivity. The (1*S*)-enantiomer of 1-substituted norcantharidin analogues showed high PP2B-selectivity. This finding provides a new approach for designing subtype-selective inhibitors. Although many researchers, including our group, have been working on the synthesis and evaluation of racemic cantharidin derivatives, the results obtained here strongly indicate that enantiomerically pure compounds, instead of racemic compounds, should be evaluated. Design and synthesis of an advanced PP2B-selective inhibitor based on these findings presented here are underway.

5. Experimental

5.1. General methods

^{1}H and ^{13}C NMR spectra were recorded on a Bruker AVANCE 500 NMR or a JEOL JNM-LA-400. Chemical shifts are reported downfield from tetramethylsilane (=0) for ^{1}H NMR. For ^{13}C NMR, chemical shifts are reported on a scale relative to the solvent used as an internal reference. Optical rotations were measured on a JASCO DIP-370 polarimeter. CD and UV spectra were recorded on JEOL J-720 WI and JEOL Ubest-V570 DS instruments, respectively. Melting points were measured using a Yanaco MP-J3. Column chromatography was performed with silica gel 60 (40–100 μm) purchased from Kanto Chemical Co. In general, reactions were carried out under anhydrous conditions in dry solvents under an argon atmosphere. Purity of the compounds obtained was determined to be more than 95%, based on ^{1}H NMR spectral analysis.

5.2. (*S*)-(−)-2-(1-Benzoyloxyethyl)furan (9) and (*R*)-(+)-2-(1-Benzoyloxyethyl)furan (6)

To a solution of (*S*)-(−)-1-(2-furyl)ethanol (413 mg, 3.69 mmol), Et_3N (771 μL, 5.53 mmol), and DMAP (45.1 mg, 0.369 mmol) in CH_2Cl_2 (20 mL) was added benzoyl chloride (514 μL, 4.43 mmol) at 0 °C, and the mixture was stirred at room temperature for 2.5 h. The reaction mixture was acidified with 1 N HCl and neutralized with saturated $NaHCO_3$. After extraction with CH_2Cl_2, the organic layer was washed with water and brine, dried over anhydrous $MgSO_4$, and concentrated in vacuo. The crude product was purified by silica gel column chromatography (10:1 hexane/EtOAc) to give (*S*)-(−)-**9** (885 mg, 92%) as a white solid.

(*S*)-**9**: mp 47–49 °C; ^{1}H NMR ($CDCl_3$, 400 MHz) δ 1.71 (d, J = 6.8 Hz, 3H), 6.22 (q, J = 6.8 Hz, 1H), 6.35 (dd, J = 3.4, 1.7 Hz, 1H), 6.40 (d, J = 3.4 Hz, 1H), 7.40–7.44 (m, 3H), 7.52–7.57 (m, 1H), 8.04 (d, J = 1.7 Hz, 1H), 8.06 (m, 1H); ^{13}C NMR ($CDCl_3$, 100 MHz) δ 18.3, 65.6, 107.9, 110.2, 128.3, 129.7, 132.9, 142.5, 153.5, 165.8; $[\alpha]_D^{20}$ −61.8 (*c* 4.14, $CHCl_3$).

(*R*)-**6** was prepared from (*R*)-(+)-1-(2-furyl)ethanol according to the same procedure. Compound **6**: $[\alpha]_D^{20}$ +60.3 (*c* 1.14, $CHCl_3$).

5.3. (1*S*,10*R*)-1-(2-Benzoyloxy)ethyl-7-oxabicyclo[2.2.1]heptane-2,3-dicarboxylic anhydride (7) and (1*R*,10*R*)-1-(2-Benzoyloxy)ethyl-7-oxabicyclo[2.2.1]heptane-2,3-dicarboxylic anhydride (8)

(*R*)-**6** (439 mg, 1.68 mmol) and maleic anhydride (247 mg, 2.52 mmol) were mixed and stirred at room temperature for 25 h. The reaction mixture was diluted with hexane/EtOAc (2:1) mixed solvent and filtered to give a diastereomixture of the Diels–Alder adducts as a white solid. The filtrate was concentrated and purified by silica gel column chromatography (5:1 hexane/EtOAc). All the Diels–Alder adducts were combined and dissolved in THF (2 mL). To this solution was added 10% Pd/C (50 mg), and the mixture was stirred at room temperature under a hydrogen atmosphere for 10 h. The reaction mixture was filtered through Celite, and concentrated in vacuo to give a diastereomixture of **7** and **8** as a white solid. The diastereomixture was purified by recrystallization (2:1 hexane/EtOAc) to give the (1*R*,10*R*)-diastereomer **8** (220 mg, 41%) as colorless crystals. The filtrate was evaporated and the residue was recrystallized from hexane–Et_2O (2:1) mixed solvent to give the (1*S*,10*R*)-diastereomer **7** (193 mg, 36%) as colorless crystals.

(1*R*,10*R*)-8: mp 192–193 °C; ^{1}H NMR ($CDCl_3$, 500 MHz) δ 1.61 (d, J = 6.5 Hz, 3H), 1.65–1.73 (m, 1H), 1.76 (ddd, J = 12.5, 12.5, 4.0 Hz, 1H), 2.02 (ddd, J = 12.5, 12.2, 5.1 Hz, 1H), 2.26 (ddd, J = 12.3, 12.3, 4.0 Hz, 1H), 3.27 (d, J = 7.5 Hz, 1H), 3.33 (d, J = 7.5 Hz, 1H), 5.01 (d, J = 5.2 Hz, 1H), 5.79 (q, J = 6.5 Hz, 1H), 7.44 (dd, J = 7.4, 7.3 Hz, 2H), 7.55 (dd, J = 7.4, 7.4 Hz, 1H), 8.02 (d, J = 7.3 Hz, 2H); ^{13}C NMR ($CDCl_3$, 125 MHz) δ 16.9, 27.8, 29.0, 51.9, 52.0, 68.0, 80.0, 91.0, 128.4 (2C), 129.7 (2C), 130.2, 133.1, 165.2, 169.0, 170.7; Anal. Calcd for $C_{17}H_{16}O_6$: C, 64.55, H, 5.10. Found: C, 64.56, H, 5.15; $[\alpha]_D^{20}$ −28.4 (*c* 1.41, $CHCl_3$).

(1*S*,10*R*)-7: mp 145–146 °C; ^{1}H NMR ($CDCl_3$, 500 MHz) δ 1.62 (d, J = 6.7 Hz, 3H), 1.73–1.82 (m,

2H), 1.83–1.92 (m, 1H), 2.03–2.12 (m, 1H), 3.29 (d, J = 7.5 Hz, 1H), 3.36 (d, J = 7.5 Hz, 1H), 5.03 (d, J = 5.4 Hz, 1H), 5.70 (q, J = 6.7 Hz, 1H), 7.45 (dd, J = 7.5, 7.3 Hz, 2H), 7.56 (dd, J = 7.5, 7.5 Hz, 1H), 8.01 (d, J = 7.3 Hz, 2H); ^{13}C NMR ($CDCl_3$, 125 MHz) δ 15.9, 29.1, 32.3, 49.8, 52.5, 69.6, 79.5, 91.9, 128.5 (2C), 129.9 (2C), 133.2 (2C), 165.4, 169.4, 170.8; Anal. Calcd for $C_{17}H_{16}O_6$: C, 64.55, H, 5.10. Found: C, 64.41, H, 5.11; $[\alpha]_D^{20}$ −36.4 (c = 0.39, $CHCl_3$).

5.4. (1*S*,10*S*)-1-(2-Benzoyloxy)ethyl-7-oxabicyclo[2.2.1]heptane-2,3-dicarboxylic anhydride (10) and (1*R*,10*S*)-1-(2-Benzoyloxy)ethyl-7-oxabicyclo[2.2.1]heptane-2,3-dicarboxylic anhydride (11)

(1*S*,10*S*)-**10** and (1*R*,10*S*)-**11** were synthesized from (*S*)-**9** according to a similar procedure to that used for (1*R*,10*R*)-**8** and (1*S*,10*R*)-**7**.

(1*S*,10*S*)-10: Anal. Calcd for $C_{17}H_{16}O_6$: C, 64.55, H, 5.10. Found: C, 64.28, H, 5.09; $[\alpha]_D^{20}$ +26.7 (c 1.37, $CHCl_3$).

(1*R*,10*S*)-11: Anal. Calcd for $C_{17}H_{16}O_6$: C, 64.55, H, 5.10. Found: C, 64.69, H, 5.11; $[\alpha]_D^{20}$ +36.5 (c 0.17, $CHCl_3$).

The UV and CD (circular dichroism) spectra of the four stereoisomers are shown in Figure 7. For preparation of enantiomerically pure 1-camphenoyloxymethyl-7-oxabicyclo[2.2.1]hept-5-ene-2,3-dicarboxylic anhydride and its CD spectra, see Ref. 15.

5.5. Compound 12

To a solution of **7** (182 mg, 0.576 mmol) and 2,4-dibromoaniline (216.8 mg, 0.864 mmol) in toluene (2 mL) were added triethylamine (160.6 μL, 1.152 mmol) and DMAP (7.1 mg, 0.058 mmol), and the mixture was stirred at 130 °C for 12 h. After removal of the solvent in vacuo, the residue was purified by silica gel column chromatography (5:1 hexane/AcOEt) to give the imide **12**. Recrystallization from benzene afforded pure **12** as colorless needles (193 mg, 61%).

^{1}H NMR ($CDCl_3$, 400 MHz) δ 1.64 (d, J = 6.6 Hz, 3H), 1.70–2.22 (m, 4H), 3.27 (d, J = 7.5 Hz, 1H), 3.29 (d, J = 7.5 Hz, 1H), 5.02 (d, J = 5.0 Hz, 1H), 5.74 (q, J = 6.6 Hz, 1H), 6.59 (d, J = 8.4 Hz, 1H), 7.22–7.44 (m, 3H), 7.52–7.57 (m, 1H), 7.82 (d, J = 2.0 Hz, 1H), 7.94 (dd, J = 8.4, 1.3 Hz, 2H); LRMS (EI) m/z 551 (M^++4), 549 (M^++2), 547 (M^+).

5.6. Protein phosphatase inhibition assays

Assays were performed according to the previously reported procedures.[4a] Phosphatases PP1 (rabbit skeletal muscle), PP2A (rabbit skeletal muscle, composed of α,β, and catalytic subunit), and PP2B (bovine brain) were purchased from UBI (Upstate Biotechnology Inc.). Protein phosphatase assays were carried out according to the UBI protocol in the presence or absence of an appropriate concentration of test compound. For PP1 and PP2A assays, a Ser/Thr Phosphatase Assay Kit 1 (UBI) was used, in which free phosphate ion released from a substrate phosphopeptide (KRpTIRR) is quantified by colorimetric analysis (630 nm) using the Malachite Green method (enzyme concentrations: 4 units/mL PP1; 56 nM PP2A). For PP2B inhibition assays, *p*-nitrophenyl phosphate (pNPP) was used as a substrate. Briefly, pNPP (2.4 mM) was incubated with PP2B (57 nM) at 37 °C (in 50 mM Tris/HCl buffer, pH 7.0, 0.1 mM $CaCl_2$, 2.5 mM $NiCl_2$, 0.3 mg/mL BSA, and 0.25 μM calmodulin) in the absence or presence of inhibitor.

5.7. Construction of binding models

To construct binding models of both enantiomers of a chiral 1-substituted norcantharidin derivative with the catalytic site of PP2B, a computational docking study was performed based on the reported PP2B-FKBP-FK506 complex structure (pdb code: 1TCO). The preliminary binding model was constructed in the Affinity module of the Insight II molecular modeling program developed by MSI (now succeeded by Accelrys, San Diego). Affinity is a program for automatically docking a ligand to a receptor using a combination of Monte Carlo type and simulated annealing procedures. The molecular mechanics program employed in Affinity is the Discover

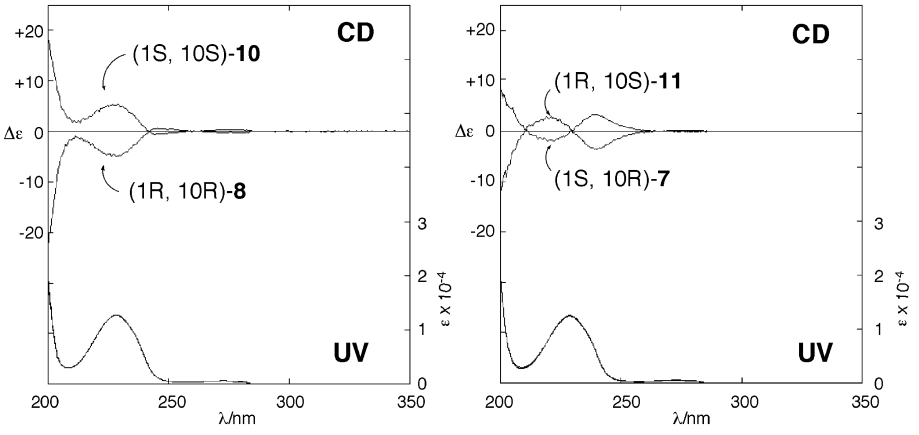

Figure 7. CD and UV spectra of chiral cantharidin analogues (**7**, **8**, **10**, and **11**) in CH_3CN.

3 module in conjunction with the force fields supported by that program. In the first orientation, we defined a subset for the binding site of the receptor, and formed an assembly consisting of the receptor and ligand molecules. The subset was defined as the amino acid residues within 7 Å around the phosphate ion, including the catalytic site of PP2B. The initial placements of norcantharidin derivatives within PP2B catalytic site were made using a Monte Carlo type procedure to search both conformational and Cartesian space. Second, a simulated annealing phase optimized each ligand placement. The structures were then subjected to energy minimization based on molecular dynamics.

Acknowledgments

We gratefully acknowledge Professors Nobuyuki Harada and Kenji Monde for measurement of CD spectra and helpful discussions. We thank Mr. Yasuharu Ijuin for X-ray analysis. We also thank Dr. Tadashi Shimizu for assistance. This work was supported in part by grants from The Naito Foundation, Suzuken Memorial Foundation, and Hoh-ansha Foundation, a SUNBOR grant, a Grant-in-Aid for Creative Scientific Research (No. 13NP0401) and a Grant-in-Aid for Scientific Research from the Japan Society for the Promotion of Science, and a Grant-in-Aid for the COE project, Giant Molecules and Complex Systems, from The Ministry of Education, Culture, Sports, Science and Technology (M.S.), as well as the Chugai Pharmaceutical Award in Synthetic Organic Chemistry (Y.B.).

References and notes

1. Wang, G. S. *J. Ethnopharmacol.* **1989**, *26*, 147–162.
2. (a) McCluskey, A. H.; Sakoff, J. A. *Mini Rev. Med. Chem.* **2001**, *1*, 43–55; (b) Li, Y.-M.; Casida, J. E. *Proc. Natl. Acad. Sci. U.S.A.* **1992**, *89*, 11867–11870; (c) Li, Y.-M.; MacKintosh, C.; Casida, J. E. *Biochem. Pharmacol.* **1993**, *46*, 1435–1443; (d) Honkanen, R. E. *FEBS Lett.* **1993**, *330*, 283–286, and references therein.
3. (a) McCluskey, A.; Taylor, C.; Quinn, R. J. *Bioorg. Med. Chem. Lett.* **1996**, *6*, 1025–1028; (b) Enz, A.; Zenke, G.; Pombo-Villar, E. *Bioorg. Med. Chem. Lett.* **1997**, *7*, 2513–2518; (c) McCluskey, A.; Keane, M. A.; Mudgee, L.-M.; Sim, A. T. R.; Sakoff, J.; Quinn, R. J. *Eur. J. Med. Chem.* **2000**, *35*, 957–964; (d) McCluskey, A.; Bowyer, M. C.; Collins, E.; Sim, A. T. R.; Sakoff, J. A.; Baldwin, M. L. *Bioorg. Med. Chem. Lett.* **2000**, *10*, 1687–1690; (e) McCluskey, A.; Walkom, C.; Bowyer, M. C.; Ackland, S. P.; Gardiner, E.; Sakoff, J. A. *Bioorg. Med. Chem. Lett.* **2001**, *11*, 2941–2946; (f) McCluskey, A.; Keane, M. A.; Walkom, C. C.; Bowyer, M. C.; Sim, A. T. R.; Young, D. J.; Sakoff, J. A. *Bioorg. Med. Chem. Lett.* **2002**, *12*, 391–393; (g) Sakoff, J. A.; Ackland, S. P.; Baldwin, M. L.; Keane, M. A.; McCluskey, A. *Invest. New Drugs* **2002**, *20*, 1–11; (h) McCluskey, A.; Sim, T. R.; Sakoff, J. A. *J. Med. Chem.* **2002**, *45*, 1151–1175; (i) Hart, M. E.; Chamberlin, R.; Wakom, C.; Sakoff, J. A.; McCluskey, A. *Bioorg. Med. Chem. Lett.* **2004**, *14*, 1969–1973; (j) Sheppeck, J. E., II; Gausss, C.-M.; Chamberlin, A. R. *Bioorg. Med. Chem.* **1997**, *5*, 1739–1750, and references cited therein.
4. (a) Baba, Y.; Hirukawa, N.; Tanohira, N.; Sodeoka, M. *J. Am. Chem. Soc* **2003**, *125*, 9740–9749; (b) Preliminary SAR results, see: Sodeoka, M.; Baba, Y.; Kobayashi, S.; Hirukawa, N. *Bioorg. Med. Chem. Lett.* **1997**, *7*, 1833–1836; (c) Tatlock, J. H.; Linton, M. A.; Hou, X. J.; Kissinger, C. R.; Pelletier, L. A.; Showalter, R. E.; Tempczyk, A.; Villafranca, J. E. *Bioorg. Med. Chem. Lett.* **1997**, *7*, 1007–1012.
5. (a) Tocci, M. J.; Matkovich, D. A.; Collier, K. A.; Kwok, P.; Dumont, F. J.; Lin, S.; Degudicibus, S.; Siekierka, J. J.; Chin, J.; Hutchison, N. I. *J. Immunol.* **1989**, *143*, 718–726; (b) Randak, C.; Brabletz, T.; Hergenrother, M.; Sobotta, I.; Serfling, E. *EMBO J* **1990**, *9*, 2529–9536; (c) Flanagan, W. M.; Corthesy, B.; Bram, R. J.; Crabtree, G. R. *Nature* **1991**, *352*, 803–807; (d) McCaffrey, P. G.; Perrino, B. A.; Soderling, T. R.; Rao, A. *J. Biol. Chem.* **1993**, *268*, 3747–3752.
6. Tsao, L. N.; Neville, C.; Musaro, A.; McCullagh, K. J. A.; Rosenthal, N. *Nat. Med.* **2000**, *6*, 2–3.
7. (a) Liu, J.; Farmer, J. D., Jr.; Lane, W. S.; Friedman, J.; Weissman, I.; Schreiber, S. L. *Cell* **1991**, *66*, 807–815; (b) Schreiber, S. L.; Albers, M. W.; Brown, E. *J. Acc. Chem. Res.* **1993**, *26*, 412–420, and references cited therein.
8. For other types of PP2B inhibitors, see: Baumgrass, R.; Weiwad, M.; Erdmann, F.; Liu, J. O.; Wunderlich, D.; Grabley, S.; Fisher, G. *J. Biol. Chem.* **2001**, *276*, 47914–47921, and references cited therein.
9. For details of our strategy for developing phosphatase inhibitors, see: (a) Sodeoka, M.; Sampe, R.; Kojima, S.; Baba, Y.; Usui, T.; Ueda, K.; Osada, H. *J. Med. Chem.* **2001**, *44*, 3216–3222; (b) Usui, T.; Kojima, S.; Kidokoro, S.; Ueda, K.; Osada, H.; Sodeoka, M. *Chem. Biol.* **2001**, *8*, 1209–1220; (c) Sodeoka, M.; Baba, Y. *J. Synth. Org. Chem. Jpn.* **2001**, *59*, 1095–1102.
10. Gausss, C.-M.; Sheppeck, J. E., II; Nairn, A. C.; Chamberlin, A. R. *Bioorg. Med. Chem.* **1997**, *5*, 1751–1773.
11. Imide derivatives of norcantharidin, which were prepared by the reaction of norcantharidin with various optically active amino acids, have been reported, but no chirality exists in the oxabicyclo[2.2.1]heptane skeleton of these compounds. See Ref. 3e.
12. Swanson, S. K.-H.; Born, T.; Zydowsky, L. D.; Cho, H.; Chang, H. Y.; Walsh, C.; Rusnak, F. *Proc. Natl. Acad. Sci. U.S.A.* **1992**, *89*, 3741–3745.
13. (a) Kissinger, C. R.; Perge, H. E.; Knighton, D. R.; Lewis, C. T.; Pelletier, L. A.; Tempczyk, A.; Kalish, V. J.; Tucker, K. D.; Showalter, R. E.; Moomaw, E. W.; Gastinel, L. N.; Habuka, N.; Chen, X.; Maldonado, F.; Barker, J. E.; Bacquet, R.; Villafranca, J. E. *Nature* **1995**, *378*, 641–644; (b) Griffith, J. P.; Kim, J. L.; Kim, E. E.; Sintchak, M. D.; Thomson, J. A.; Fitzgibbon, M. J.; Fleming, M. A.; Caron, P. R.; Hsiao, K.; Navia, M. A. *Cell* **1995**, *82*, 507–522.
14. Goldberg, J.; Huang, H. B.; Kwon, Y. G.; Greengard, P.; Nairn, A. C.; Kuriyan, J. *Nature* **1995**, *376*, 745–753; Crystal structure of PP1-calyculin complex, see:Kita, A.; Matsunaga, S.; Takai, A.; Kataiwa, H.; Wakimoto, T.; Fusetani, N.; Isobe, M.; Miki, K. *Structure* **2002**, *10*, 715–724.
15. Theurillat-Moritz, V.; Vogel, P. *Tetrahedron: Asymmetry* **1996**, *7*, 3163–3168.